



HAL
open science

Chondrocytes Play a Major Role in the Stimulation of Bone Growth by Thyroid Hormone

Clémence Desjardin, Cyril Charles, Catherine Benoist-Lasselin, Julie Riviere, Maïlys Gilles, Olivier Chassande, Caroline Morgenthaler, Denis Laloë, Jérôme Lecardonnell, Frederic Flamant, et al.

► **To cite this version:**

Clémence Desjardin, Cyril Charles, Catherine Benoist-Lasselin, Julie Riviere, Maïlys Gilles, et al.. Chondrocytes Play a Major Role in the Stimulation of Bone Growth by Thyroid Hormone. *Endocrinology*, 2014, 155 (8), pp.3123-3135. 10.1210/en.2014-1109 . hal-01193997

HAL Id: hal-01193997

<https://hal.science/hal-01193997>

Submitted on 27 May 2020

HAL is a multi-disciplinary open access archive for the deposit and dissemination of scientific research documents, whether they are published or not. The documents may come from teaching and research institutions in France or abroad, or from public or private research centers.

L'archive ouverte pluridisciplinaire **HAL**, est destinée au dépôt et à la diffusion de documents scientifiques de niveau recherche, publiés ou non, émanant des établissements d'enseignement et de recherche français ou étrangers, des laboratoires publics ou privés.

Chondrocytes Play a Major Role in the Stimulation of Bone Growth by Thyroid Hormone

Clémence Desjardin, Cyril Charles, Catherine Benoist-Lasselain, Julie Riviere, Mailys Gilles, Olivier Chassande, Caroline Morgenthaler, Denis Laloé, Jérôme Lecardonnell, Frédéric Flamant, Laurence Legeai-Mallet, and Laurent Schibler

Institut National de la Recherche Agronomique (INRA) (C.D., J.R., M.G., C.M., D.L., J.L., L.S.), UMR1313, Biologie Intégrative et Génétique Animale, Jouy-en-Josas, France; Centre National de la Recherche Scientifique (CNRS) UMR 5242 (C.C.), ENS Lyon, Institut de Génomique Fonctionnelle, Université de Lyon, Lyon, France; Institut Imagine (C.B.-L., L.L.-G.) Institut National de la Santé et de la Recherche Médicale, U1163, Université Paris Descartes, 75015 Paris, France; University of Bordeaux (O.C.), U1026, Bioingénierie Tissulaire, Bordeaux, France; and Institut de Génomique Fonctionnelle de Lyon (F.F.), Université de Lyon, CNRS, INRA, École Normale Supérieure de Lyon, 69364 Lyon Cedex 07, France

Thyroid hormone (T_3) is required for postnatal skeletal growth. It exerts its effect by binding to nuclear receptors, TRs including $TR\alpha 1$ and $TR\beta 1$, which are present in most cell types. These cell types include chondrocytes and osteoblasts, the interactions of which are known to regulate endochondral bone formation. In order to analyze the respective functions of T_3 stimulation in chondrocytes and osteoblasts during postnatal growth, we use *Cre/loxP* recombination to express a dominant-negative $TR\alpha 1^{L400R}$ mutant receptor in a cell-specific manner. Phenotype analysis revealed that inhibiting T_3 response in chondrocytes is sufficient to reproduce the defects observed in hypothyroid mice, not only for cartilage maturation, but also for ossification and mineralization. $TR\alpha 1^{L400R}$ in chondrocytes also results in skull deformation. In the meantime, $TR\alpha 1^{L400R}$ expression in mature osteoblasts has no visible effect. Transcriptome analysis identifies a number of changes in gene expression induced by $TR\alpha 1^{L400R}$ in cartilage. These changes suggest that T_3 normally cross talks with several other signaling pathways to promote chondrocytes proliferation, differentiation, and skeletal growth. (*Endocrinology* 155: 3123–3135, 2014)

The skeleton is made up of bones developing through 2 distinct processes, intramembranous and endochondral ossification. Intramembranous ossification, which occurs in the calvarial bones and distal clavicles, involves direct differentiation of mesenchymal cells into osteoblasts. In contrast, endochondral ossification, which occurs in the remainder of the skeleton, involves differentiation of mesenchymal cells into chondrocytes that form a cartilage template for future bone. During endochondral ossification, chondrocytes undergo hypertrophic differentiation, characterized by sequential changes in cell morphology and matrix synthesis, and the cartilage is ultimately

replaced by bone tissue following vascular invasion. This process progression is tightly regulated by numerous circulating hormones, cytokines, and growth factors (1, 2) including thyroid hormone T_3 (the active derivative of T_4).

Childhood hypothyroidism results in short stature, bone age delay, skeletal dysplasia, and delayed dental development, with abnormally thin growth plates and impaired chondrocyte hypertrophy (3). Hypothyroid rats display a disorganized growth plate with a decreased hypertrophic zone (4). Conversely, childhood thyrotoxicosis accelerates growth and advances bone age. It also induces

ISSN Print 0013-7227 ISSN Online 1945-7170

Printed in U.S.A.

Copyright © 2014 by the Endocrine Society

Received February 6, 2014. Accepted June 3, 2014.

First Published Online June 10, 2014

Abbreviations: Thyroid hormone (TH), $TR\alpha 1$, thyroid hormone receptor $\alpha 1$; μ CT, micro-CT; BMD, bone mineral density; BV/TV, bone volume fraction; ECM, extracellular matrix; 3D, 3-dimensional.

For News & Views see page 2747

short stature due to premature fusion of the growth plates (5). T_3 is thus a positive regulator of cartilage maturation, stimulating the clonal expansion of resting chondrocytes and their subsequent hypertrophic differentiation. This correlates with changes in glycosaminoglycan secretion and the induction of collagen X expression (6–8).

These actions are either direct or mediated through interactions with other signaling pathways. In particular, T_3 has been shown to control or interact with pathways involved in the pace of chondrocyte proliferation and differentiation, including the *Ihh*–*PTHrP*, *GH*, *IGF1*, *Wnt*, *BMPs*, and fibroblast growth factors (*FGFs*) (9). Likewise, T_3 has been shown to stimulate osteoblast biosynthetic activity and differentiation through key pathways including *IGF1*, *FGF receptor 1*, and *RANKL* (9).

T_3 exerts its effect by binding to nuclear receptors (TRs). In mice, the 2 main receptors, $TR\alpha$ 1 and $TR\beta$ 1 are encoded by the *Thra* and *Thrb* genes, which are both expressed in chondrocytes, osteoblasts, and osteoclasts. Unliganded TRs repress target gene transcription by recruiting corepressors. Upon T_3 binding, they change their conformation, dissociating from the corepressor complex and recruiting transcription coactivators. This results in transactivation of neighboring genes.

In humans, germline mutations of either *THRA* (10, 11) or *THRB* (12) have multiple detrimental consequences, which comprise delayed bone growth and short stature. In mice, the knock-out and knock-in mutations of *Thra* and *Thrb* also have a visible effect on skeletal growth. Because *Thrb* mutations result in increased circulating levels of TSH and T_3 due to disruption of the hypothalamic-pituitary-thyroid axis, the bone phenotype of the corresponding mutant mice resembles skeletal hyperthyroidism, with advanced ossification and increased mineralization. Their bone phenotype does not reflect the absence of $TR\beta$ 1-mediated response of bone cells, but rather the excess of circulating T_3 acting via $TR\alpha$ 1 (13–17). By contrast, *Thra* mutations do not markedly alter the serum level of T_3 and lead to a delayed ossification and bone growth that resembles hypothyroidism. Therefore the local function of $TR\alpha$ 1 seems to be predominant in bone growth, consistent with the 10-fold higher mRNA levels of $TR\alpha$ than $TR\beta$ 1 in the skeleton (16). However, in one of the *Thra* knock-in models, growth is only delayed and adult mice reach normal size (18).

In order to investigate the specific and direct roles of $TR\alpha$ 1 in cartilage maturation and bone ossification, we used Cre-mediated recombination in mice to generate tissue-specific *Thra* mutations from a floxed allele called $TR\alpha^{AMI}$ (for AF2-mutation, inducible). The allele design is such that Cre recombination leads to the expression of a mutant receptor, $TR\alpha^{L400R}$, unable to interact with

histone acetyl transferase coactivators. The expression of the nonreceptor isoforms encoded by *Thra* (19) remains unchanged. $TR\alpha^{L400R}$ exerts a dominant-negative activity, preventing T_3 response of heterozygous cells. Although in vitro experiments suggest that the dominant-negative activity can also affect $TR\beta$ 1, in vivo studies suggest that $TR\beta$ 1 functions are preserved (20). In the present study, we crossed mice carrying the $TR\alpha^{AMI}$ allele with transgenic mice expressing Cre either in chondrocytes and their progenitors (*Col2Cre*) or in mature osteoblasts (*Col1Cre*). Phenotype analysis and molecular studies revealed that, during early phases of skeletal development, the main function of $TR\alpha$ 1 is to stimulate chondrocyte differentiation. Thus, alterations of bone structure observed in hypothyroidism are likely to result, at least in part, from a primary defect in cartilage maturation.

Materials and Methods

Animals

The $TR\alpha^{AMI}$ construction has been extensively studied previously (20–23). *Col1Cre* mice (24) and were obtained from the Mutant Mouse Regional Resource Center (MMRRC) at the University of California, Davis. *Col2Cre* mice have also been fully characterized (25), and we verified that transgene expression per se does not alter bone growth or adult size. Tissue specificity of Cre expression was further confirmed by PCR in a panel of 8 tissues (data not shown). $TR\alpha^{AMI/AMI}$ males (129/Sv) were crossed with *Col2Cre^{tg/wt}* or *Col1Cre^{tg/wt}* females (C57Bl6 background) to produce control mice ($TR\alpha^{AMI/wt}$ *Col2Cre^{w/wt}* and $TR\alpha^{AMI/wt}$ *Col1Cre^{w/wt}*) and mutant mice expressing the dominant-negative $TR\alpha^{L400R}$ protein in cartilage or bone ($TR\alpha^{L400R/wt}$ *Col2Cre^{tg/wt}* and $TR\alpha^{L400R/wt}$ *Col1Cre^{tg/wt}*, thereafter called $TR\alpha^{L400R}/C2$ and $TR\alpha^{L400R}/C1$; Supplemental Figure 1). At least 3 pairs of mice (males and/or females) were generated for subsequent analysis at postnatal days 7, 14, 21, 28, and 35 (P7, P14, P21, P28, P35). The experimental protocol number 12/033 was reviewed and approved by the Animal Care Committee of INRA and AgroParisTech (COMETHEA, France), which abides by the requirements of Directive 86/609 of the European Community Council. Blood samples were collected from P14, P21, and P28 to estimate T_3/T_4 circulating levels using Roche T_3 and T_4 ECLIA Electrochemiluminescence assay. We verified a posteriori that the phenotypes of male and female bone were not statistically different for all measured parameters.

Histomorphometry and in situ hybridization

$TR\alpha^{L400R}/C2$ femurs from P1, P14, and P28 mice were fixed for 24 hours in paraformaldehyde and decalcified in 0.5M EDTA buffer for 1–3 weeks. Paraffin-embedded 5- μ m longitudinal sections were stained with hematoxylin-eosin or alcian blue-alizarin red. In situ hybridizations were performed using type II and type X collagen probes to identify resting (RZ), proliferative (PZ), and hypertrophic zones (HZ) of the growth plate. Image J software was used to calculate mean values for the epiphysis and

ossification center area as well as growth plate thickness and RZ, PZ, and HZ heights in femur sections. Four to 6 animals per genotype were examined at each time point. At least 2 different levels of section were examined for each sample by taking at least 5 separate measurements across each section examined.

For histomorphometry analyses of $TR\alpha^{L400R}/C1$, long bones were fixed, dehydrated at 4°C, and embedded in methyl-methacrylate (26). For each right femur or tibia, 7- μ m thick longitudinal sections, parallel to the sagittal plane, were analyzed. Histomorphometric analysis was performed using the NIS-Elements AR software (Nikon). The measured trabecular area encompassed the secondary spongiosa, trabecular bone perimeter, and single- and double-labeled perimeters, and interlabeled widths were measured. These were used to calculate MS/BS ([double labeled perimeters + single labeled perimeters]/trabecular perimeters), mineral apposition rate ([interlabeled widths/interval time]), bone formation rate ([double labeled perimeters + single labeled perimeters]/2) \times interlabeled widths/interval time/trabecular perimeters). All statistical comparisons were done using Student's *t* test.

X-Ray and X-ray microcomputed tomography (μ CT) analysis

The skeletons of the $TR\alpha^{L400R}/C2$ mice and their control littermates were radiographed on Kodak oncology film using Cabinet X-ray System Faxitron series-Hewlett Packard (15 seconds, 35 kV, and 3 mA). Mouse femurs were stored in 70% ethanol at 4°C before μ CT analysis. Scans were performed using 5 μ m voxel for femurs and 14–17 μ m for heads (Phoenix nanotom, GE measurement and control). The scanner used a tungsten source X-ray tube operating at 100 kV and 70 μ A. Images were reconstructed using Phoenix datos x 2 CT software. The Microview software was used for measurements, and the calibration for mineral density in the scans was performed with use of a phantom (hydroxyapatite). For each sample, 2 regions of interest were designed manually and scanned, corresponding to the trabecular subchondral bone area (2-mm region below the cartilage) and to the cortical bone area (measured 5 mm under the cartilage area). The morphometric parameters examined were bone mineral density (BMD), bone mineral content (BMC), tissue mineral content (TMC), tissue mineral density (TMD), bone volume fraction (BV/TV), relative bone surface (BS/BV), trabecular thickness (Tb.Th), trabecular number (Tb.N), and trabecular separation (Tb.Sp). For cortical bone, the parameters measured were BMD, inner and outer perimeters, marrow and cortical areas, and total area.

For the femurs of 14-week-old $TR\alpha^{L400R}/C1$ mice, 3-dimensional (3D) microarchitecture of the distal femur was evaluated using a high-resolution (8 μ m) microtomographic imaging system (eXplore Locus, General Electric). A 3D region within the secondary spongiosa in the proximal metaphysis of the tibia or femur was reconstructed, beginning 500 μ m proximal to the growth plate and extending to 1.5 mm. Trabecular bone volume fraction (BV/TV, %) was determined using the Advanced Bone Analysis (ABA) software (General Electric). Skulls scans of P14 to P35 $TR\alpha^{L400R}/C2$ were performed using 14–17 μ m voxel. Geometric morphometric analyses were performed using Amira 5.3 and MorphoJ softwares with 36 3D landmarks defined on skulls and mandibles. Specimen size was normalized, and land-

marks from different specimens were superimposed using the Procrustes method.

Transcriptome analysis

Three pairs of male mutant and control littermates, as well as 3 pairs of female mutant and control littermates were analyzed using Agilent SurePrint G3 Mouse Gene Expression microarrays. The 2 femoral heads were collected and immediately frozen in liquid nitrogen. Samples were crushed frozen using a mortar and pestle, and RNA extraction was performed using QIAGEN RNeasy Mini kit. RNA amplification and labeling were performed using the one-color Low Input Quick Amp Labeling kit (Agilent Technologies). Each RNA sample (50 ng) was amplified and cyanin 3 (Cy3) labeled. Subsequently, cRNA (600 ng) was fragmented and used for hybridization on Agilent sureprint G3 Mouse GE 8 \times 60K Microarrays (design ID: 028005). Scans (G2505CA; Agilent Technologies) were at a resolution of 3 μ m and a dynamic range of 20 bits. The resulting images were analyzed using the Feature Extraction software version 7.10.3.1 (Agilent Technologies). Statistical analyses were done in the BioConductor version 2.10 (27) and R version 2.15.0 environments. To identify genes that were differentially expressed, we applied the empirical Bayes on normalized data, moderated *t*-statistics implemented in the BioConductor package LIMMA (version 3.12.0) (28). *P* values were adjusted for multiple testing using the Benjamini and Hochberg method.

Results

Expression of $TR\alpha^{L400R}$ in mature osteoblasts has no visible effect on postnatal growth and long bones ossification

To clarify the respective contribution of mature osteoblasts and chondrocytes to the promotion of bone growth by T_3 , we generated 2 transgenic mouse models expressing the $TR\alpha^{L400R}$ mutant receptor in one of these 2 cell types ($TR\alpha^{L400R}/C1$ and $TR\alpha^{L400R}/C2$, respectively). In both cases, mice were born in the expected Mendelian ratios, and their global health was not visibly affected. We first observed the phenotype of $TR\alpha^{L400R}/C1$ mice, expressing the mutation in mature osteoblasts. No macroscopic defect was visible in these mice. We used X-ray μ CT to analyze ossification at P14 and did not find any difference between mutant mice and control littermates in BMD, bone volume, trabecular volume, or other morphologic parameters (Supplemental Table 1). We also analyzed bone structure at adult stage (14 weeks) within the secondary spongiosa in the proximal metaphysis of the tibia or femur and performed 3D reconstruction. Calcein labeling (2 days before analysis) was used to assess bone remodeling dynamic parameters, and staining for tartrate-resistant alkaline phosphatase activity was used to evaluate osteoclast activity. None of these investigations revealed any obvious influence of the mutation on bone structure and development (data not shown). This led us

to conclude that altering of $T_3/TR\alpha 1$ signaling in mature osteoblasts is not sufficient to alter bone growth, and that another cell type, most likely chondrocyte, must play a major role in the T_3 stimulation of bone growth.

Expression of $TR\alpha 1^{L400R}$ in chondrocytes results in postnatal growth retardation and delayed ossification

Based on morphometric and bone length comparative analyses, $TR\alpha^{L400R}/C2$ mice had important and persistent postnatal growth retardation. $TR\alpha^{L400R}/C2$ mice were 20% smaller and 25% lighter compared with the control at all postnatal ages examined (Figure 1 and Supplemental Table 2). Mutant femurs, tibias, humeri, and ulnas as well as paws were 20% shorter than bones from control animals at all examined stages. However, the $TR\alpha^{L400R}/C2$ mice phenotype remained harmonious.

X-ray imaging and μ CT analysis revealed delayed ossification in $TR\alpha^{L400R}/C2$ mice (Figure 2A). This was confirmed by alcian blue/alizarin red skeletal preparations, showing a greater proportion of blue-stained cartilage in the mutant appendicular and axial skeleton (humerus,

tibia, vertebrae, and ribs) at P14, P21 and P28 (data not shown). Vertebrae of mutant mice were shorter and undermineralized (Figure 2B). More strikingly, epiphyses were not visible in the tibias and femurs of mutant mice both at P14 (Figure 2C) and P35 (Figure 2, B and D). Altogether, our results show that $TR\alpha^{L400R}/C2$ mice display growth retardation by 2–3 weeks associated with a delayed ossification. As expected, T_3 and T_4 circulating levels showed no systemic alteration (Supplemental Table 3), confirming that the observed effects are cell-autonomous consequences of $TR\alpha 1^{L400R}$ expression in chondrocytes.

Expression of $TR\alpha 1^{L400R}$ in chondrocytes leads to skull abnormalities due to impaired endochondral ossification

$TR\alpha^{L400R}/C2$ mice showed a macroscopic abnormal skull conformation with a shorter snout and minor incisor malocclusion (Figure 1A). A 10% significant difference in length and width of skull between control and mutant mice was observed (Supplemental Table 2). Detailed μ CT analysis of the skull further revealed important modifications, including an incomplete mineralization of supraoccipital bone at 5 weeks of age (Figure 3A). There was an occipital gap in the $TR\alpha^{L400R}/C2$ skulls. This phenotype is indicative of a delayed development of the occipital bones. Interestingly, the affected parts correspond to a structure of cartilaginous origin, which is not yet mineralized after birth (29). There was a normal persistence of cartilage at spheno-occipital and intraoccipital synchondrosis in $TR\alpha^{L400R}/C2$ mice compared with controls. There was no premature fusion of the sutures in mutant mice.

A morphometric analysis performed on skulls of P14, P21, and P35 mice allowed analysis of allometric growth by performing principal component analysis (PCA). For the skull, the first PCA axis, which is highly correlated with age ($P < .0001$), corresponded to a progressive elongation of the skull, especially for the snout (Figure 3B). Segregation of control and $TR\alpha^{L400R}/C2$ growth lines on the analysis clearly indicates that the skull shape is modified in

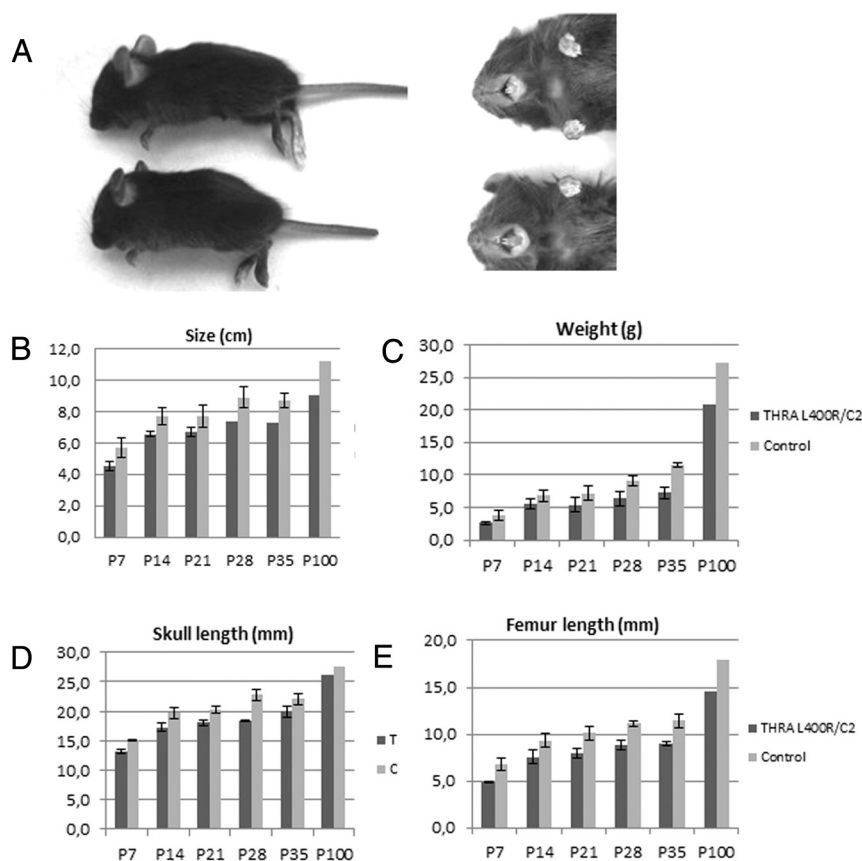


Figure 1. $TR\alpha 1^{L400R}$ mutation in chondrocytes result in permanent size reduction: (A) Mutant mice exhibit an important and persistent postnatal growth retardation and minor incisor malocclusion (upper panel). B–E, Statistical analysis (Student t-tests) of indicated parameters reveal a significant reduction (20%) in global size, femur and skull length, and weight in $TR\alpha^{L400R}/C2$ mice which is maintained in adults.

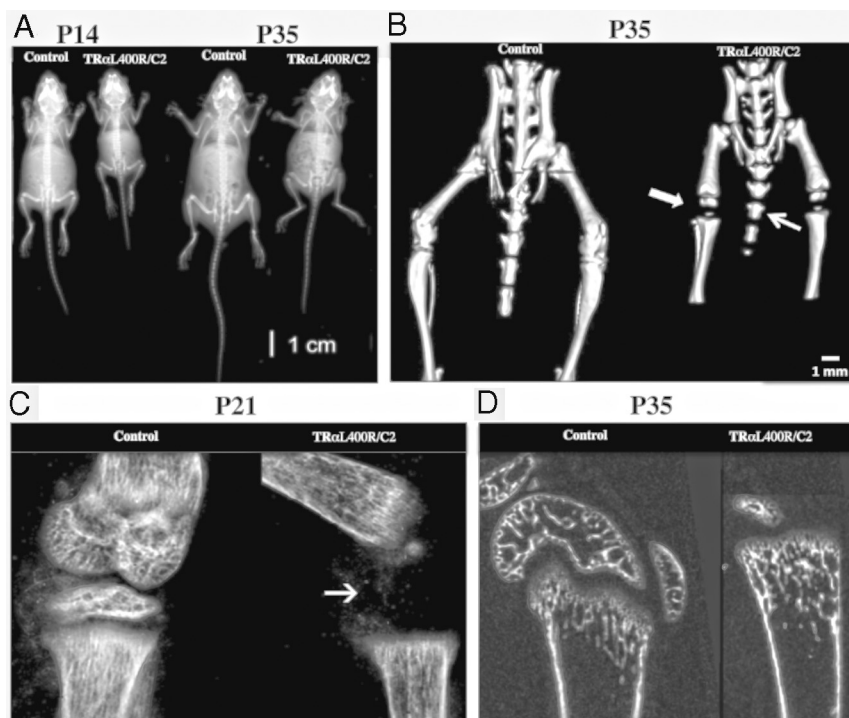


Figure 2. 3D and X-ray imaging indicates dwarfism and bone age delay in $TR\alpha^{L400R}/C2$ mice. (A)- X-ray at P14 and P35 (B)- 3D imaging confirmed the delay of ossification (arrows) at P35. C, -High magnification at the level of the knee confirming the ossification delay in $TR\alpha^{L400R}/C2$ mice at P21 (arrows). D, Ossification delay at P35 (arrows).

mutants from early stages. Coordinates of mutant specimens along PCA axis 1 indicate a retarded growth, with an important delay at P35, in $TR\alpha^{L400R}/C2$ mice. The second PCA axis appeared to be uncorrelated with age ($P = .65$) and represented shape modification of the lower distal part of the skull. The apparent shift of growth lines along this second axis suggested a reduction of the supraoccipital area of the neurocranium. In contrast, study of mandibular shape revealed only minor differences between mutants and controls (Figure 3C), corresponding to a reduction in size of the angular process. Because the abnormal skull morphology apparently results from defects in cartilage-derived bone growth, we conclude that it is due to impaired endochondral, but not intramembranous, ossification.

Expression of $TR\alpha^{L400R}$ in chondrocytes impairs cartilage maturation and alters trabecular bone structure

Comparison of the growth plate organization for $TR\alpha^{L400R}/C2$ and control mice at P7, P15, P21, and P28 was based on histology (Figure 4) and in situ hybridization of mRNA encoding type-II collagen, type X collagen, osteocalcin, and osteopontin (Figure 5). This confirmed a 2- to 3-week delay for the formation of a secondary ossification center in the epiphysis of $TR\alpha^{L400R}/C2$ mice. By contrast, no difference was observed at any of these de-

velopmental stages for *VEGF* expression, a gene encoding a growth factor known to play a major part in coupling angiogenesis and osteogenesis in mineralized cartilage and bony trabeculas (data not shown).

In good agreement with these observations, histomorphometry showed a dramatic change in the ossification center area in mutant $TR\alpha^{L400R}/C2$ long bones (OC/GPO ratio in Figure 6). In addition, we observed a 20% lower femur epiphysis height (Supplemental Table 4). Growth plate (GP) as well as proliferative zone and hypertrophic zone height were measured, showing a 10%–15% lower GP height due to a narrowing of both PZ (–10%) and HZ (–15%) (Figure 6). During growth, control and mutant GP seemed to evolve in a similar way, except that the HZ, which declines with age, appeared to be slower for mutant mice between 2 and 4 weeks.

Noteworthy, lower GP height appeared to be proportionate to the smaller size of the femur epiphysis.

The rate of chondrocyte proliferation, decreased over time in both controls and $TR\alpha^{L400R}/C2$ PZ. The decrease was accelerated in mutant mice, resulting in a significant reduction in bromodeoxyuridine incorporation in mutant chondrocytes at P7 and P14, but not at P21, compared with controls (Figure 7 and Supplemental Table 5). However, immunohistochemistry for cell cycle markers, using antibodies directed against Cyclin D1, p21, and p57, did not reveal any difference between mutants and controls at these developmental stages (data not shown).

As seen above (Figure 5C), osteocalcin expression was lost in the epiphysis area and in trabeculas of subchondral bone, suggesting an impairment in the bone mineralization process. To more directly address this point, μ CT was used to analyze subchondral and cortical bone properties (Figure 8 and Supplemental Table 6). Lower BMD and trabecular thickness were observed in femoral subchondral bone of $TR\alpha^{L400R}/C2$ mice. In addition, an increase in trabecular number was observed at P14. The lower BMD was the result of a decreased tissue mineral density, and not of bone volume fraction, suggesting that the quality, but not the volume, of the mineralized bone was altered in mutant mice. Noteworthy, subchondral bone parameters of P35 $TR\alpha^{L400R}/C2$ mice appeared similar to

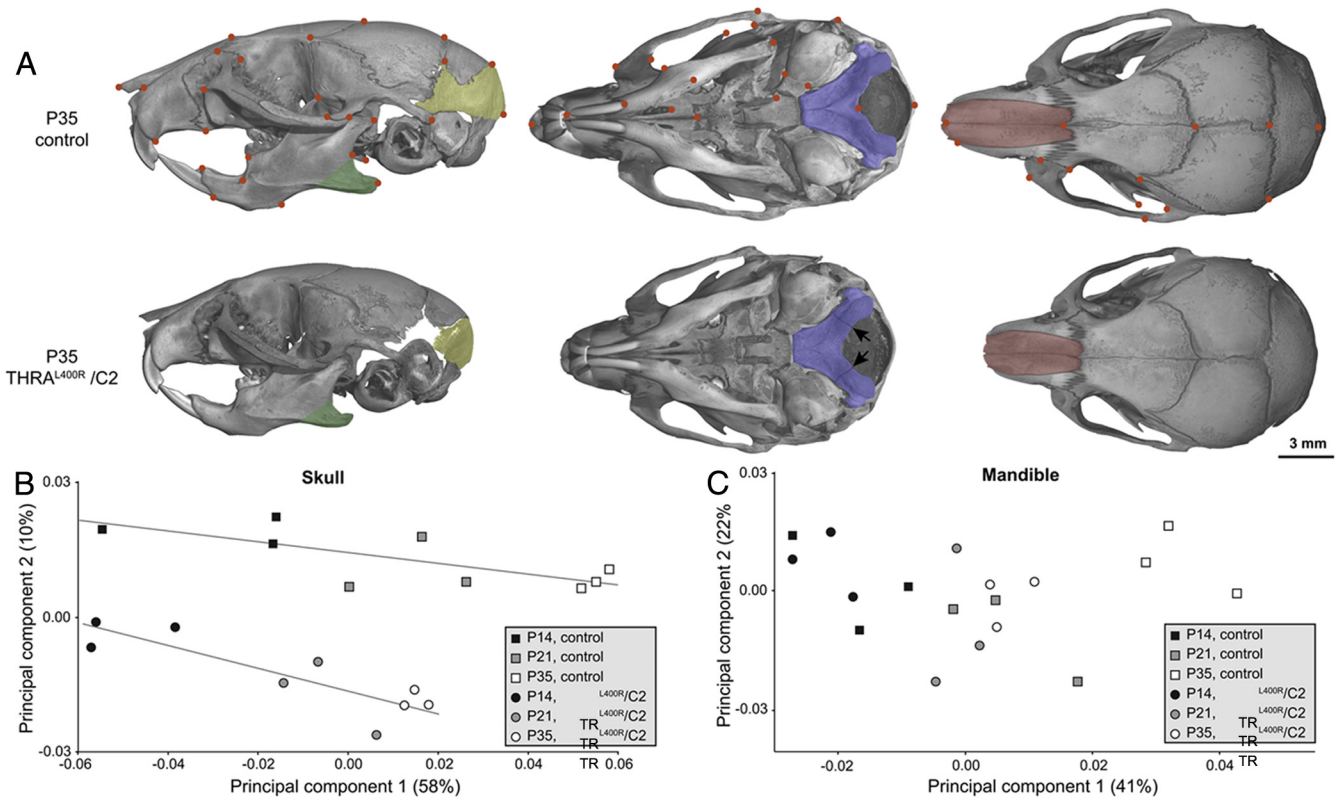


Figure 3. Morphological modifications in skulls and mandibles caused by the expression of TR α 1^{L400R} in chondrocytes. A. Comparison of TR α 1^{L400R}/C2 and control mice at P35. Arrows indicate the unfused intra-occipital suture in TR α 1^{L400R}/C2 mice. B-C Plot of principal components 1 and 2 based on Procrustes analysis of skull (B) and mandibular (C) 3D landmark coordinates of TR α 1^{L400R}/C2 and control mice at P14, P21 and P35.

the ones of P21 controls, as illustrated by PCA analysis (Supplemental Figure 2), confirming that the overall process of bone mineralization is greatly delayed. In cortical bone, the reduced cortical area in mutants suggested a possible imbalance between bone formation by osteoblasts of periosteum and endosteum and bone resorption by osteoclasts in the endosteum.

Gene deregulation alterations induced by TR α 1^{L400R} expression in chondrocytes

To investigate the molecular mechanisms underlying the TR α 1^{L400R}/C2 phenotype defects, and to identify the immediate consequences of expressing TR α 1^{L400R} in chondrocytes, we performed cartilage transcriptome analysis at P14. DNA from 6 pairs of TR α 1^{L400R}/C2 mutant and

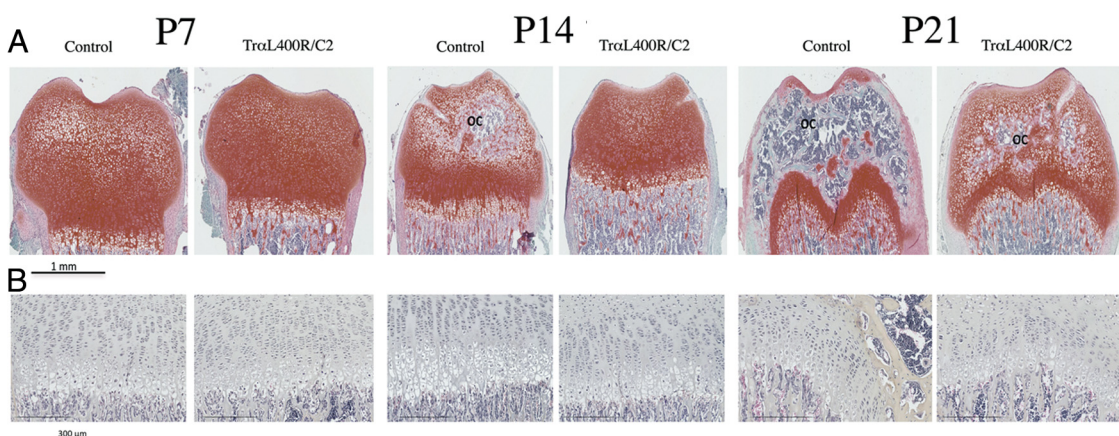


Figure 4. Delay of ossification in TR α 1^{L400R}/C2 femurs. A, Light green-Safranin O staining of control and TR α 1^{L400R}/C2 femurs showing a delay of the formation of the epiphyseal ossification center (OC) in the mutant at P14 and P21. B, Histological analyses of the growth plate showing a reduction of the size of the growth plate from P7 to P21.

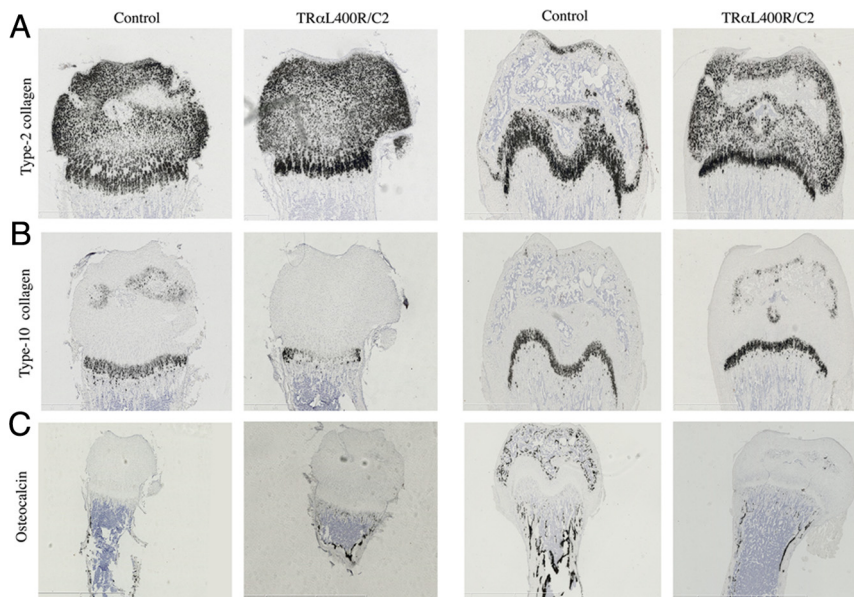


Figure 5. Expression of TR $\alpha 1^{L400R}$ in chondrocytes alter both chondrocytes and osteoblasts populations in femurs (A) In situ hybridization of *Col2a1*, encoding type II collagen showing a specific expression restricted to the cartilage. B, In situ hybridization of *Col10a1*, encoding type X collagen does not indicate any significant change in the hypertrophic zone in TR $\alpha^{L400R}/C2$ mice. C, In situ hybridization of *Bglab* encoding osteocalcin in osteoblasts, shows a specific expression in the mineralized tissues and confirms a delay of bone maturation.

control littermates (3 pairs of males and 3 pairs of females) were analyzed using Agilent SurePrint G3 Mouse Gene Expression microarrays. This analysis highlighted 95 down-regulated and 361 up-regulated genes in mutant mice (fold change superior to 1.5, adjusted *P* value ≤ 0.05) (Supplemental Table 7). We used quantitative PCR to confirm some of these observations (Supplemental Table 8).

Gene Ontology (GO) analysis indicated that these genes are mainly involved in development (including 47 genes involved in skeletal development) cellular organization, cell communication, metabolic processes (including nucleic acid and protein metabolism as well as proteoglycan biosynthesis and bone mineralization), cell adhesion, vesicle-mediated transport, cell cycle, and apoptosis (Supplemental Table 9).

These modulated genes are associated with several skeletal phenotypes such as abnormal birth body size (MP:0009701) and skeleton morphology (MP:0005508), as well as abnormal bone ossification (MP:0008271). Statistically enriched biological processes include cell differentiation (GO:0030154), regulation of biosynthetic process (GO:0009889), regulation of primary metabolic process (GO:0080090), especially regulation of RNA metabolic process (GO:0051252) and regulation of nitrogen compound metabolic process (GO:0051171), as well as cell adhesion (GO:0007155) and cilium morphogenesis (GO:0060271) (Supplemental Table 7).

Noteworthy, increased expression of *Igf1r* ($\times 1.9$) and *Igf2r* ($\times 1.7$) was observed, whereas no change in *Ghr* and *Fgfr3* expression could be detected.

Discussion

The generation of somatic mutations by *Cre/loxP* recombination reveals that TR $\alpha 1$ in cartilage plays a predominant role in the promotion of bone growth by T₃. In agreement with previous study (17) this leaves little room for the controversial hypothesis that proposed an indirect influence of TSH (30). Although our data suggest that T₃ only acts on chondrocytes, and not in osteoblasts, it should be stressed that in the TR $\alpha^{L400R}/C1$ mice, TR $\alpha 1^{L400R}$ is only expressed at a late stage of osteoblast differentiation. Therefore, the possibility remains that the

T₃/TR $\alpha 1$ pathway is also required at early steps of their differentiation. Similarly, we did not explore a possible bone homeostasis alteration linked to aging in our models. However, our genetic evidence confirms previous hypotheses based on in vitro studies (31) and phenotype analysis of mice carrying germ line mutations (32, 33) that attribute to chondrocytes a pivotal role in the promotion of bone growth and ossification by T₃. This developmental function appears to be mediated mainly by TR $\alpha 1$.

Comparison with other *Thra* knock-in mouse models

The bone phenotype has been reported for mice expressing mutations similar to TR $\alpha 1^{L400R}$. The TR $\alpha 1^{PV}$ mutation (34) also alters the C-terminal helix required for the ligand-dependent recruitment of coactivators, whereas the TR $\alpha 1^{R384C}$ mutation reduces ligand affinity (18). The bone phenotype of TR $\alpha 1^{PV/+}$ and TR $\alpha 1^{R384C/+}$ mice is also marked by a major delay in endochondral ossification (32, 35). In both cases, a proportional narrowing of PZ and HZ was observed, reflecting impaired entry of progenitor cells into the PZ, together with impaired hypertrophic chondrocyte differentiation. In our study we found, however, that the PZ evolves similarly in mutants and controls up to P30, whereas the HZ declines at a slower rate in mutants between P15 and P30. This rather suggests a differential effect of TR $\alpha 1^{L400R}$ expres-

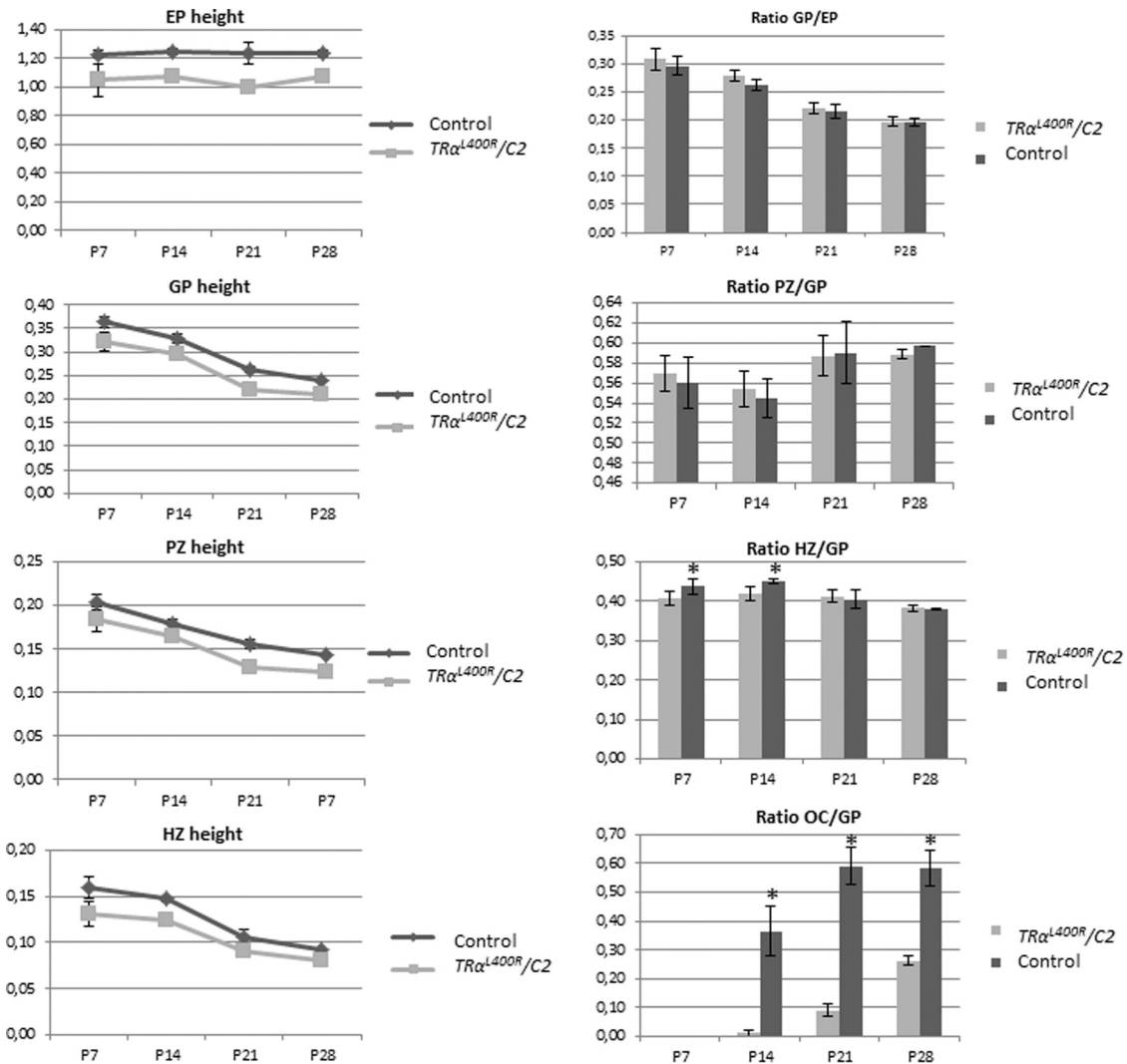


Figure 6. Expression of $TR\alpha^{L400R}$ in chondrocytes delays endochondral ossification. Histomorphometric analysis of the growth plate showing that the heights of epiphysis (EP), growth plate (GP), proliferative zone (PZ) and hypertrophic zone (HZ) were reduced in $THR\alpha^{L400R}/C2$ mice compared to control littermates. Ratio calculations indicate a proportionate reduction of GP height compared to femur size, and a relative reduction in the size of EP, PZ and HZ. The ratio OC/GP confirmed a delay in endochondral ossification.

sion on proliferative and hypertrophic chondrocytes during growth.

Another discrepancy is that $TR\alpha^{PV/+}$ and $TR\alpha^{R384C/+}$ mice display delayed intramembranous ossification of the skull (delayed fontanel closure and suture fusion), without apparent change in skull dimension, whereas we observed a modification in skull shape consistent with impaired endochondral ossification without alteration in intramembranous ossification. The observed defect in $TR\alpha^{L400R}/C2$ snout elongation also leads to incisor malocclusion, which is likely to modify forces produced by masseter muscles attached to the angular process. Because angular process development is partly dependent on such forces (36), it is tempting to speculate that the primary defect of supraoccipital bone may cause small changes in mandible shape, whereas disruption of

the Meckel cartilage may alter both size and shape of the mandible.

One likely explanation for these differences is that the $TR\alpha^{PV}$ and $TR\alpha^{R384C}$ are expressed in all cell types. Therefore delayed intramembranous ossification, as observed in these mice, is unlikely to be a cell-autonomous consequence of mutant receptor expression in chondrocytes. It is possible, however, that the dissimilarities between the mouse models result from differences in receptor conformations. Three human mutations in the *THRA* gene have been reported recently, altering the C-terminal helix of the receptor like the mouse PV and L400R mutations (10, 11, 37, 38). The patients with these mutations share a number of phenotypic alterations, including short stature, macrocephaly, and bone age delay but also display marked differences: For example,

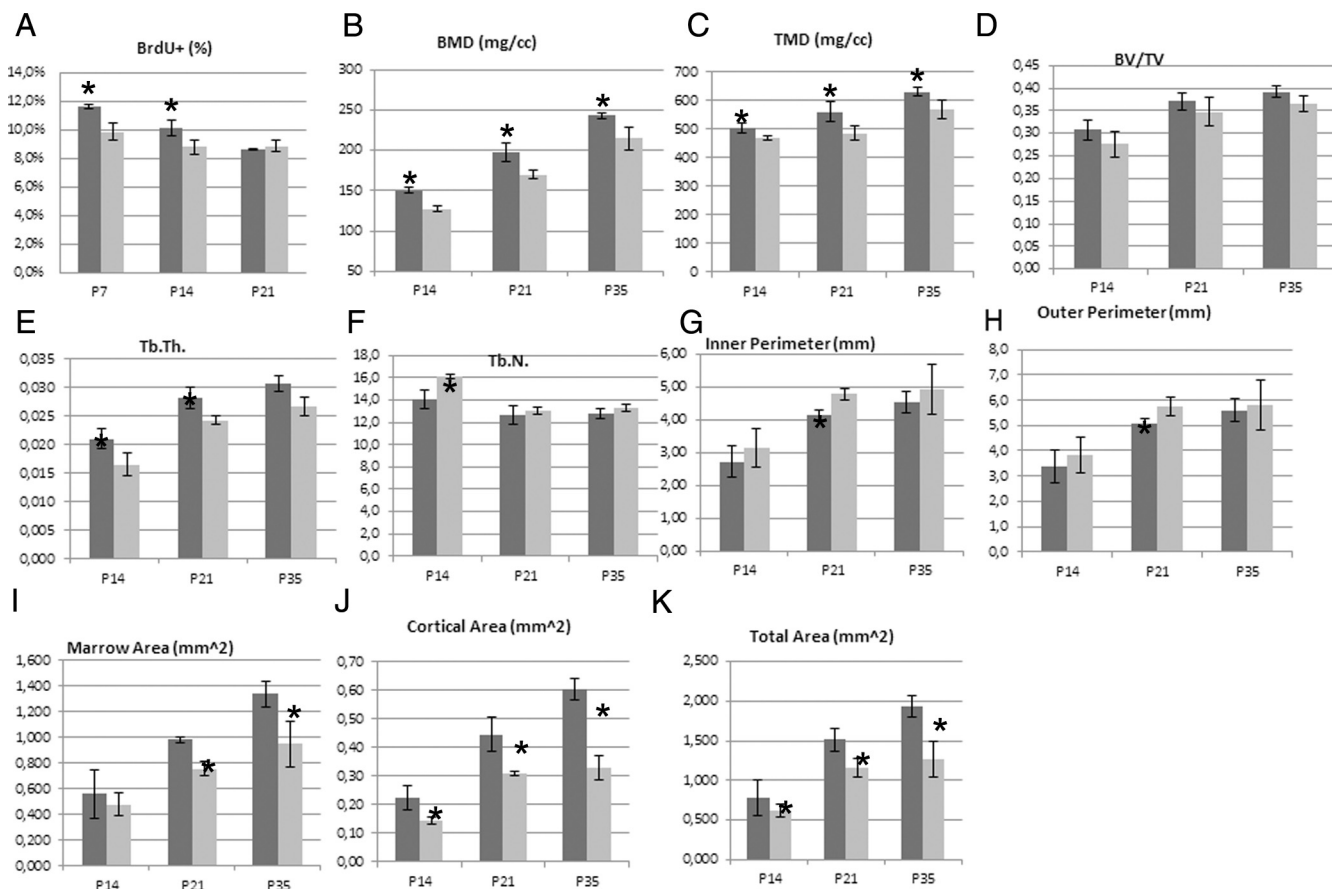


Figure 7. Expression of $TR\alpha^{L400R}$ in chondrocytes decreases chondrocyte proliferation and alters bone structure. A) BrdU labeling reveals a significant lower rate of chondrocyte proliferation in the femur growth plate at P7 and P14 in mutants. B-L) Microcomputed tomography (μ CT) analysis of femurs in $TR\alpha^{L400R/C2}$ mice. Subchondral trabecular bone display a lower BMD and TMD (B and C) at P14, P21 and P35. The BV/TV ratio (D) is not significantly altered. The trabecular thickness is also lower in mutant mice and the number of trabeculae is lower at P14 (E and F). Taken together, these results suggest that the lower BMD results from a delay of mineralization in mutant mice but that the volume of the mineralized bone is not altered. There are significant differences between the cortical bone of control and mutant mice for the inner and the outer perimeters (G,H) and for the cortical and marrow areas (I,J). These data suggest an impaired balance between bone formation by osteoblasts of the periosteum and endosteum and bone resorption by osteoclasts in the endosteum.

dysgenesis and fragmentation of the femoral epiphysis were reported in 2 of 4 cases only (10). It seems therefore that different *THRA* mutations may produce variable phenotypes. A similar situation has been reported for *THRB* mutations, for which extensive *in vitro* studies showed that similar changes in receptor structures can have different outcomes (39).

Role of $TR\alpha 1$ in cartilage

T_3 seems to act in cartilage at several levels. It stimulates the clonal expansion of resting chondrocytes and inhibits chondrocyte proliferation. It also stimulates hypertrophic chondrocyte differentiation, as shown by induction of collagen X expression, changes in heparan sulfate proteoglycan secretion, and alkaline phosphatase activity upon T_3 stimulation (40, 41). Likewise, T_3 is involved in terminal differentiation and capillary invasion by stimulating the degradation of proteoglycans, as illustrated by the aggre-

can breakdown induced by T_3 enhancement of aggrecanase-2/ADAM-TS5 activity (42).

The respective functions of $TR\alpha 1$ and $TR\beta 1$ in these processes are still unclear. In primary culture of rib chondrocytes, T_3 treatment decreases cell proliferation. This *in vitro* effect is mediated by $TR\beta 1$, not $TR\alpha 1$ (31), and is linked to a stimulation of BMP signaling (43). This is in apparent contradiction to the phenotype of mice with the *Thrb* mutation, which have advanced bone age. However, these mice have impaired pituitary-thyroid axis and elevated T_3 level, and their bone phenotype mainly reflects excessive $TR\alpha 1$ stimulation by T_3 (16, 32). In our study, a 5%-15% decrease in chondrocyte proliferation rate was found in $TR\alpha^{L400R}/C2$ mice, suggesting that $TR\alpha 1$ may be involved in mediating a positive effect of T_3 on chondrocyte proliferation, as observed in other cell types (44–46). However, our study does not arrive at a firm conclusion concerning the respective contribution of $TR\alpha 1$ and

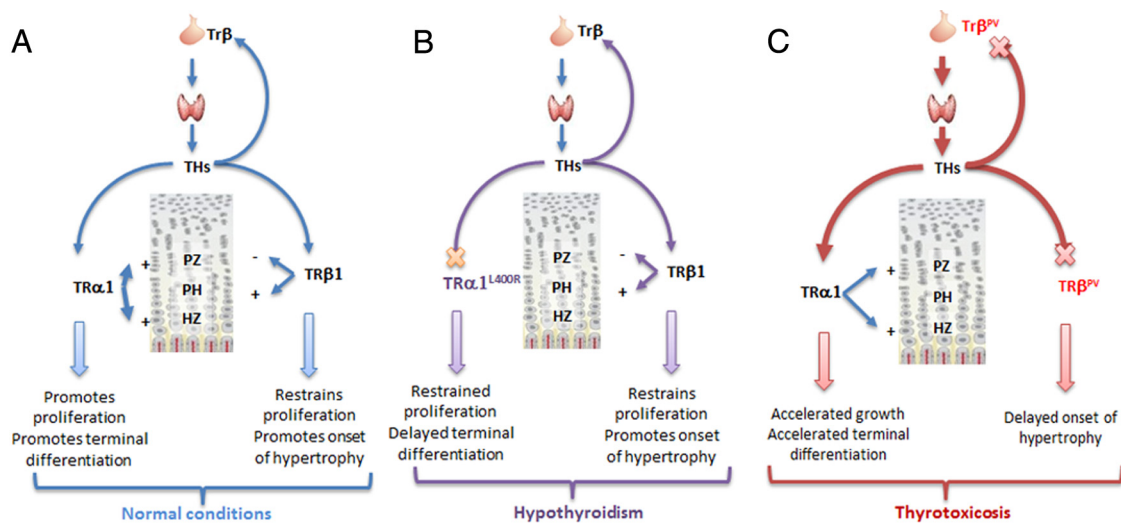


Figure 8. A unifying model for the role of TR α in cartilage and bone development. TR β mutations alter bone growth mainly in an indirect manner, by altering the feedback regulation of the circulating T₃ level and creating a status of thyrotoxicosis. TR α 1 mutations produce a phenotype similar to hypothyroidism, by preventing chondrocytes of the hypertrophic and proliferation zone to respond to T₃ stimulation. Modified from (9).

TR β 1. The reason is that we cannot rule out that the TR α 1^{L400R} mutated receptor exerts its dominant-negative activity on both TR α 1 and TR β 1. However, a systematic analysis of mice expressing TR α 1^{L400R} in all tissues indicates that most known *Thrb* functions are preserved (20).

Extracellular matrix (ECM) alterations and cross talks with other signaling pathways

We expected that our transcriptome analysis would clarify the functions of T₃ in cartilage maturation. One limitation is that changes in mRNA levels may not reflect the direct influence of TR1^{L400R} on gene expression in chondrocytes but instead changes in the cellular composition of the cartilage at P14. These changes in cellular composition are illustrated by our in situ hybridization results, which indicate a strong reduction in the number of cells containing *Bglab* mRNA, which encodes osteocalcin. This decrease is unlikely to reflect down-regulation of *Bglab* expression but most likely relates to the reduced number of osteoblasts located in the femoral head, due to the delayed secondary ossification process. The cellular heterogeneity of the studied sample also explains why we did not capture the changes in gene expression associated with the reduced proliferation, because we would expect that only a small fraction of proliferating chondrocytes would display differential expression for cell-cycle genes. The only observed changes for this gene category were for *Ccnh* encoding cyclin H ($\times 1.6$ in TR α ^{L400R}/C2 mice) and *Cdc26* ($\times 1.8$).

Despite these limitations, some of the changes revealed by transcriptome analysis should correspond to direct TR target genes and are likely to play a causative role in the

observed phenotype, whereas others are secondary consequences of altered cell differentiation status. We tried to recognize some of the direct target genes by comparing our dataset with similar transcriptome analysis performed in other tissues (47–49) and by using the genome-wide TR occupancy data recently performed in a neural cell line (50). We expected that at least some of the target genes would be shared by different cell types. This was not the case. It seems therefore that, as previously reported for other nuclear receptors, the repertoire of TR target genes differs widely between different cell types.

One striking outcome of our transcriptome analysis is the observation of major changes in expression for genes involved in ECM biosynthesis, structure, and dynamics. Only a few of these genes (*Bcan* [2.2]) and *Gpc3* [$\times 1.9$]) encode structural components of ECM. Changes in gene expression were more frequently related to biosynthesis and catabolism of ECM. For example, down-regulation of *Mmp10* (2.8) may impair proteoglycan degradation. Likewise, up-regulation of *Csgalnact1* ($\times 2.3$) and *Chst13* ($\times 1.7$), which are involved in chondroitin sulfate synthesis and sulfation, and *Hyal2* ($\times 1.8$), which is essential for the breakdown of hyaluronan, may lead to a disruption of ECM biomechanical properties. In good agreement with a previous study (41), up-regulation of *Hs6st2* ($\times 1.7$) was also observed, suggesting changes in heparin sulfate sulfation pattern that may alter its biological functions. Among these functions are the stabilization of aggrecans and the sequestration and diffusion of several growth factors such as FGFs and Indian Hedgehog. These changes in ECM may thus impact numerous signaling

pathways known to influence chondrocyte proliferation and differentiation.

Our data also suggest cross talks between T_3 signaling and other signaling pathways. For example *Smoc1* ($\times 1.8$), encodes a known BMP antagonist. A complex situation was observed with respect to the IGF1 pathway. Up-regulations were observed in mutant cartilage for *Igf1r* ($\times 1.9$), *Igf2r* ($\times 1.7$), *Igf2bp2* ($\times 1.6$). T_3 has already been shown to stimulate *Igf1r* expression in cultured cells (51). Increasing the level of receptor for IGF-1 should contribute to stimulate the proliferation of resting-zone chondrocytes, increase chondrocyte hypertrophy, and promote longitudinal bone growth (52). The increase in *igf1r* expression is thus paradoxical, considering the observation of reduced bone growth in mutant mice. This apparent inconsistency suggests that up-regulation of some inhibitors exert a predominant influence. For instance, *Wisp3* ($\times 2.6$) has been demonstrated to suppress IGF1 signaling in chondrocytes and to be part of a WISP3–IGF1 regulatory loop whereby *Wisp3* restricts IGF1-mediated chondrocyte hypertrophy (53). Likewise, *Igf2bp2* is known to counteract IGF1 signaling (54). Alternatively, reduced bone growth may result from an impaired cross talk with the Wnt-catenin signaling pathways, which have been shown to act downstream of IGF1 signaling to stimulate growth plate chondrocyte proliferation and promote hypertrophy (51). Up-regulation of genes encoding Wnt antagonist (*Sfrp1* $\times 2.4$ and *Sfrp2* $\times 2$) and frizzled receptors (*Fzd2* $\times 1.9$; *Fzd9* $\times 2$) should result in decreased proliferation and altered chondrocytes differentiation, in a manner similar to the one previously reported for the intestinal epithelium (45, 55, 56). In addition, *Sox9* ($\times 2.7$) is known to restrict Wnt signaling (57) and its overexpression in mouse chondrocytes results in a delayed endochondral ossification (58). Furthermore, Wnt and several other signaling pathways depend largely upon the cytoskeleton and ciliary signaling (59). Interestingly, deregulation of cytoskeleton, primary cilium, and cell adhesion represent other striking features emerging from our data. The role of cell shape and cell-cell and cell-ECM interactions, all relying on the cytoskeleton, as well as ciliary signaling are now well recognized and considered as essential to the maturation of chondrocytes (60).

Delayed ossification in mutant mice results primarily from the growth plate impairment, in good agreement with previous studies suggesting that impaired chondrocyte terminal differentiation may be responsible for defective bone development (61, 62). Our microarray analysis may also provide clues on the indirect consequences of impaired chondrocyte proliferation and differentiation on vascular invasion, osteoblast and osteoclast recruitment, and mineralization. In this respect, we identified several

down-regulated chemokines (*Ccl3* 2.4, *Ccl4* 1.6, *Ccl9* 2.3, and *Ccl12* 1.6) and secreted proteins (*Bglab* encoding osteocalcin 12.5, *Ostn* encoding osteocrin 2.2 and *Wisp2* 2.2) that may correspond to these defective processes. In addition to their role in angiogenesis (63–65) chemokines play a role in bone maturation. They favor osteoclastogenesis (osteocalcin, CCL9) (66, 67) and osteoclast resorption function (osteocalcin, CCL3) (68, 69). Furthermore, CCL4 is thought to play a role in maturation and function of osteoblasts (70), and osteocrin acts as a soluble inhibitor of osteoblast differentiation (71).

In summary, $TR\alpha 1^{L400R}$ has 2 effects on chondrocyte differentiation. It first refrains their proliferation. It impairs neither the onset of chondrocyte hypertrophy nor the hypertrophic process per se but then alters the fine tuning of terminal differentiation, leading to delayed ossification (Figure 9). Impaired chondrocyte terminal differentiation is then responsible for a defective vascularization and/or osteoblast recruitment, leading to a delayed development of the secondary ossification center. This phenotype is very similar to the one reported in hypothyroidism, suggesting that the ability of T_3 to promote chondrocyte proliferation and terminal differentiation plays a critical role in its ability to promote skeletal growth.

Acknowledgments

We thank Dr Mallein-Gerin from Institute of Biology and Chemistry of Proteins (LBTi, CNRS-LIMR 5305, Lyon) for providing the *Col2Cre* mouse model and Suzy Markossian for technical help.

Address all correspondence and requests for reprints to: Frederic Flamant, PhD, Ecole Normale Supérieure de Lyon – IGFL, 46 Allée d'Italie, Lyon – 69007, France. E-mail: Frederic.Flamant@ens-lyon.fr.

Author Contribution: Study design: L.S. Study conduct: C.D., L.S., L.L.M., and F.F. Data collection: C.D., J.R., C.M., C.B.L., C.C., O.C., J.L.C. Data analysis and interpretation: L.S., C.D., L.L.M., F.F., D.L., C.C., O.C. Manuscript writing and revising: L.S., C.D., L.L.M., F.F., and O.C.

This study was funded, in part, by a starting grant from INRA Animal genetics Department and UMR1313 GABI and EuroGrow (FP6-LSHM-CT-2007-037471). This work was supported by the Thyrogenomic2 ANR grant (to F.F.).

Disclosure Summary: All authors have nothing to disclose.

References

1. Marino R. Growth plate biology: new insights. *Curr Opin Endocrinol Diabetes Obes.* 2011;18(1):9–13.
2. Mackie EJ, Tatarczuch L, Mirams M. The skeleton: a multi-functional complex organ: the growth plate chondrocyte and endochondral ossification. *J Endocrinol.* 2011;211(2):109–121.

3. Williams GR, Robson H, Shalet SM. Thyroid hormone actions on cartilage and bone: interactions with other hormones at the epiphyseal plate and effects on linear growth. *J Endocrinol.* 1998;157(3):391–403.
4. Stevens DA, Harvey CB, Scott AJ, et al. Thyroid hormone activates fibroblast growth factor receptor-1 in bone. *Mol Endocrinol.* 2003;12:12.
5. Schlesinger B, Fisher OD. Accelerated skeletal development from thyrotoxicosis and thyroid overdosage in childhood. *Lancet.* 1951;2(6677):289–290.
6. Robson P, Wright GM, Keeley FW. Distinct non-collagen based cartilages comprising the endoskeleton of the Atlantic hagfish, *Myxine glutinosa*. *Anat Embryol.* 2000;202(4):281–290.
7. Miura Y, Takahashi T, Jung SM, Moroi M. Analysis of the interaction of platelet collagen receptor glycoprotein VI (GPVI) with collagen. A dimeric form of GPVI, but not the monomeric form, shows affinity to fibrous collagen. *J Biol Chem.* 2002;277(48):46197–46204.
8. Bassett JH, Williams GR. The molecular actions of thyroid hormone in bone. *Trends Endocrinol Metab.* 2003;14(8):356–364.
9. Wojcicka A, Bassett JH, Williams GR. Mechanisms of action of thyroid hormones in the skeleton. *Biochim Biophys Acta.* 2013;1830(7):3979–3986.
10. Bochukova E, Schoenmakers N, Agostini M, et al. A mutation in the thyroid hormone receptor α gene. *N Engl J Med.* 2012;366(3):243–249.
11. van Mullem AA, Chrysis D, Eythimiadou A, et al. Clinical phenotype of a new type of thyroid hormone resistance caused by a mutation of the TR α 1 receptor: consequences of LT4 treatment. *J Clin Endocrinol Metab.* 2013;98(7):3029–3038.
12. Weiss RE, Refetoff S. Resistance to thyroid hormone. *Rev Endocr Metab Disord.* 2000;1(1–2):97–108.
13. Bassett JH, O'Shea PJ, Chassande O, et al. Analysis of skeletal phenotypes in thyroid hormone receptor mutant mice. *Scanning.* 2006;28(2):91–93.
14. O'Shea PJ, Bassett JH, Cheng SY, Williams GR. Characterization of skeletal phenotypes of TR α 1 and TR β mutant mice: implications for tissue thyroid status and T3 target gene expression. *Nucl Recept Signal.* 2006;4:e011.
15. O'Shea PJ, Bassett JH, Cheng SY, Williams GR. Characterization of skeletal phenotypes of TR α 1 and TR β mutant mice: implications for tissue thyroid status and T3 target gene expression. *Nucl Recept Signal.* 2006;4:e011.
16. O'Shea PJ, Harvey CB, Suzuki H, et al. A thyrotoxic skeletal phenotype of advanced bone formation in mice with resistance to thyroid hormone. *Mol Endocrinol.* 2003;17(7):1410–1424.
17. Bassett JH, O'Shea PJ, Sriskantharajah S, et al. Thyroid hormone excess rather than thyrotropin deficiency induces osteoporosis in hyperthyroidism. *Mol Endocrinol.* 2007;21(5):1095–1107.
18. Tinnikov A, Nordström K, Thorén P, et al. Retardation of postnatal development caused by a negatively acting thyroid hormone receptor α 1. *Embo J.* 2002;21(19):5079–5087.
19. Flamant F, Samarut J. Thyroid hormone receptors: lessons from knockout and knock-in mutant mice. *Trends Endocrinol Metab.* 2003;14(2):85–90.
20. Quignodon L, Vincent S, Winter H, Samarut J, Flamant F. A point mutation in the activation function 2 domain of thyroid hormone receptor α 1 expressed after CRE-mediated recombination partially recapitulates hypothyroidism. *Mol Endocrinol.* 2007;21(10):2350–2360.
21. Fauquier T, Romero E, Picou F, et al. Severe impairment of cerebellum development in mice expressing a dominant-negative mutation inactivating thyroid hormone receptor α 1 isoform. *Dev Biol.* 2011;356(2):350–358.
22. Picou F, Fauquier T, Chatonnet F, Flamant F. A bimodal influence of thyroid hormone on cerebellum oligodendrocyte differentiation. *Mol Endocrinol.* 2012;26(4):608–618.
23. Fauquier T, Chatonnet F, Picou F, et al. Purkinje cells and Bergmann glia are primary targets of the TR α 1 thyroid hormone receptor during mouse cerebellum postnatal development. *Development.* 2014;141(1):166–175.
24. Dacquin R, Starbuck M, Schinke T, Karsenty G. Mouse α 1(I)-collagen promoter is the best known promoter to drive efficient Cre recombinase expression in osteoblast. *Dev Dyn.* 2002;224(2):245–251.
25. Sakai K, Hiripi L, Glumoff V, et al. Stage- and tissue-specific expression of a Col2a1-Cre fusion gene in transgenic mice. *Matrix biology: journal of the International Society for Matrix Biology.* 2001;19(8):761–767.
26. Parfitt AM. Bone histomorphometry: standardization of nomenclature, symbols and units. Summary of proposed system. *Bone Miner.* 1988;4(1):1–5.
27. Gentleman RC, Carey VJ, Bates DM, et al. Bioconductor: open software development for computational biology and bioinformatics. *Genome Biol.* 2004;5(10):R80.
28. Smyth GK, Michaud J, Scott HS. Use of within-array replicate spots for assessing differential expression in microarray experiments. *Bioinformatics.* 2005;21(9):2067–2075.
29. Guihard-Costa AM, Sakka M. [Variations as a function of time of the ossification of various bony elements of the cranial vault (experimental study in mice)]. *Bulletin de l'Association des anatomistes.* 1986;70(211):27–32.
30. Abe E, Marians RC, Yu W, et al. TSH is a negative regulator of skeletal remodeling. *Cell.* 2003;115(2):151–162.
31. Rabier B, Williams AJ, Mallein-Gerin F, Williams GR, Chassande O. Thyroid hormone-stimulated differentiation of primary rib chondrocytes in vitro requires thyroid hormone receptor β . *J Endocrinol.* 2006;191(1):221–228.
32. O'Shea PJ, Bassett JH, Sriskantharajah S, Ying H, Cheng SY, Williams GR. Contrasting skeletal phenotypes in mice with an identical mutation targeted to thyroid hormone receptor α 1 or β . *Mol Endocrinol.* 2005;19(12):3045–3059.
33. Monfoulet LE, Rabier B, Dacquin R, et al. Thyroid hormone receptor β mediates thyroid hormone effects on bone remodeling and bone mass. *J Bone Miner Res.* 2011;26(9):2036–2044.
34. Kaneshige M, Suzuki H, Kaneshige K, et al. A targeted dominant negative mutation of the thyroid hormone α 1 receptor causes increased mortality, infertility, and dwarfism in mice. *Proc Natl Acad Sci USA.* 2001;98(26):15095–15100.
35. Bassett JH, Nordström K, Boyde A, et al. Thyroid status during skeletal development determines adult bone structure and mineralization. *Mol Endocrinol.* 2007;21(8):1893–1904.
36. Rot-Nikcevic I, Downing KJ, Hall BK, Kablar B. Development of the mouse mandibles and clavicles in the absence of skeletal myogenesis. *Histology and histopathology.* 2007;22(1):51–60.
37. Moran C, Schoenmakers N, Agostini M, et al. An adult female with resistance to thyroid hormone mediated by defective thyroid hormone receptor α . *J Clin Endocrinol Metab.* 2013;98(11):4254–61.
38. van Mullem A, van Heerebeek R, Chrysis D, et al. Clinical phenotype and mutant TR α 1. *N Engl J Med.* 2012;366(15):1451–1453.
39. Collingwood TN, Adams M, Tone Y, Chatterjee VK. Spectrum of transcriptional, dimerization, and dominant negative properties of twenty different mutant thyroid hormone β -receptors in thyroid hormone resistance syndrome. *Mol Endocrinol.* 1994;8(9):1262–1277.
40. Robson H, Siebler T, Stevens DA, Shalet SM, Williams GR. Thyroid hormone acts directly on growth plate chondrocytes to promote hypertrophic differentiation and inhibit clonal expansion and cell proliferation. [In Process Citation]. *Endocrinology.* 2000;141(10):3887–3897.
41. Bassett JH, Swinhoe R, Chassande O, Samarut J, Williams GR. Thyroid hormone regulates heparan sulfate proteoglycan expression in the growth plate. *Endocrinology.* 2006;147(1):295–305.
42. Makihira S, Yan W, Murakami H, et al. Thyroid hormone enhances

- aggrecanase-2/ADAM-TS5 expression and proteoglycan degradation in growth plate cartilage. *Endocrinology*. 2003;144(6):2480–2488.
43. Lassová L, Niu Z, Golden EB, Cohen AJ, Adams SL. Thyroid hormone treatment of cultured chondrocytes mimics in vivo stimulation of collagen X mRNA by increasing BMP 4 expression. *J Cell Physiol*. 2009;219(3):595–605.
 44. Trentin AG. Thyroid hormone and astrocyte morphogenesis. *J Endocrinol*. 2006;189(2):189–197.
 45. Kress E, Samarut J, Plateroti M. Thyroid hormones and the control of cell proliferation or cell differentiation: paradox or duality? *Mol Cell Endocrinol*. 2009;313(1–2):36–49.
 46. Kowalik MA, Perra A, Pibiri M, et al. TR β is the critical thyroid hormone receptor isoform in T3-induced proliferation of hepatocytes and pancreatic acinar cells. *J Hepatol*. 2010;53(4):686–692.
 47. Gil-Ibañez P, Morte B, Bernal J. Role of thyroid hormone receptor subtypes α and β on gene expression in the cerebral cortex and striatum of postnatal mice. *Endocrinology*. 2013;154(5):1940–1947.
 48. Chan IH, Privalsky ML. Isoform-specific transcriptional activity of overlapping target genes that respond to thyroid hormone receptors α 1 and β 1. *Mol Endocrinol*. 2009;23(11):1758–1775.
 49. Lin JZ, Sieglaff DH, Yuan C, et al. Gene specific actions of thyroid hormone receptor subtypes. *PLoS One*. 2013;8(1):e52407.
 50. Chatonnet F, Guyot R, Benoît G, Flamant F. Genome-wide analysis of thyroid hormone receptors shared and specific functions in neural cells. *Proc Natl Acad Sci U S A*. 2013;110(8):E766–E775.
 51. Wang L, Shao YY, Ballock RT. Thyroid hormone-mediated growth and differentiation of growth plate chondrocytes involves IGF-1 modulation of β -catenin signaling. *J Bone Miner Res*. 2010;25(5):1138–1146.
 52. van der Eerden BC, Karperien M, Wit JM. Systemic and local regulation of the growth plate. *Endocr Rev*. 2003;24(6):782–801.
 53. Repudi SR, Patra M, Sen M. WISP3-IGF1 interaction regulates chondrocyte hypertrophy. *J Cell Sci*. 2013;126(Pt 7):1650–1658.
 54. Firth SM, Baxter RC. Cellular actions of the insulin-like growth factor binding proteins. *Endocr Rev*. 2002;23(6):824–854.
 55. Kress E, Rezza A, Nadjar J, Samarut J, Plateroti M. The frizzled-related sFRP2 gene is a target of thyroid hormone receptor α 1 and activates β -catenin signaling in mouse intestine. *J Biol Chem*. 2009;284(2):1234–1241.
 56. Kress E, Skah S, Sirakov M, et al. Cooperation between the thyroid hormone receptor TR α 1 and the WNT pathway in the induction of intestinal tumorigenesis. *Gastroenterology*. 2010;138(5):1863–1874.
 57. Topol L, Chen W, Song H, Day TF, Yang Y. Sox9 inhibits Wnt signaling by promoting β -catenin phosphorylation in the nucleus. *J Biol Chem*. 2009;284(5):3323–3333.
 58. Akiyama H. [Transcriptional regulation in chondrogenesis by Sox9]. *Clin Calcium*. 2011;21(6):845–851.
 59. May-Simera HL, Kelley MW. Cilia, Wnt signaling, and the cytoskeleton. *Cilia*. 2012;1(1):7.
 60. Woods A, Wang G, Beier F. Regulation of chondrocyte differentiation by the actin cytoskeleton and adhesive interactions. *J Cell Physiol*. 2007;213(1):1–8.
 61. Lu C, Wan Y, Cao J, et al. Wnt-mediated reciprocal regulation between cartilage and bone development during endochondral ossification. *Bone*. 2013;53(2):566–574.
 62. Mugniery E, Dacquin R, Marty C, et al. An activating Fgfr3 mutation affects trabecular bone formation via a paracrine mechanism during growth. *Hum Mol Genet*. 2012;21(11):2503–2513.
 63. Sahin H, Borkham-Kamphorst E, Kuppe C, et al. Chemokine Cxcl9 attenuates liver fibrosis-associated angiogenesis in mice. *Hepatology*. 2012;55(5):1610–1619.
 64. Wu Y, Li YY, Matsushima K, Baba T, Mukaida N. CCL3-CCR5 axis regulates intratumoral accumulation of leukocytes and fibroblasts and promotes angiogenesis in murine lung metastasis process. *J Immunol*. 2008;181(9):6384–6393.
 65. Tsui P, Das A, Whitaker B, et al. Generation, characterization and biological activity of CCL2 (MCP-1/JE) and CCL12 (MCP-5) specific antibodies. *Hum Antibodies*. 2007;16(3–4):117–125.
 66. Yang M, Mailhot G, MacKay CA, Mason-Savas A, Aubin J, Odgren PR. Chemokine and chemokine receptor expression during colony stimulating factor-1-induced osteoclast differentiation in the toothless osteopetrotic rat: a key role for CCL9 (MIP-1 γ) in osteoclastogenesis in vivo and in vitro. *Blood*. 2006;107(6):2262–2270.
 67. Hashimoto F, Kobayashi Y, Mataka S, Kobayashi K, Kato Y, Sakai H. Administration of osteocalcin accelerates orthodontic tooth movement induced by a closed coil spring in rats. *European journal of orthodontics*. 2001;23(5):535–545.
 68. Taddei SR, Queiroz-Junior CM, Moura AP, et al. The effect of CCL3 and CCR1 in bone remodeling induced by mechanical loading during orthodontic tooth movement in mice. *Bone*. 2013;52(1):259–267.
 69. Roach HI. Why does bone matrix contain non-collagenous proteins? The possible roles of osteocalcin, osteonectin, osteopontin and bone sialoprotein in bone mineralisation and resorption. *Cell Biol Int*. 1994;18(6):617–628.
 70. Hoshino A, Iimura T, Ueha S, et al. Deficiency of chemokine receptor CCR1 causes osteopenia due to impaired functions of osteoclasts and osteoblasts. *J Biol Chem*. 2010;285(37):28826–28837.
 71. Thomas G, Moffatt P, Salois P, et al. Osteocrin, a novel bone-specific secreted protein that modulates the osteoblast phenotype. *J Biol Chem*. 2003;278(50):50563–50571.